Influence of the 11 year solar cycle on annual streamflow maxima in Southern Canada

Andreas Prokoph [a], Jan Adamowski [b,*], Kaz Adamowski [c]

[a] Department of Earth Sciences, University of Ottawa, Ottawa, ON, Canada K1N 6N5
[b] Department of Bioresource Engineering, McGill University, 21 111 Lakeshore Road, Ste. Anne de Bellevue, QC, Canada H9X 3V9
[c] Department of Civil Engineering, University of Ottawa, Ottawa, ON, Canada K1N 6N5

ARTICLE INFO

SUMMARY

The re-occurrence pattern of major extremes in hydrology, such as the timing and intensity of river floods, is related to a variety of natural and anthropogenic factors. In this study, the particular temporal regional influence of ~11 year solar radiation cyclicities on the maximum annual streamflow (MAS) records from six stations from four eco-zones in Southern Canada were investigated. Wavelet analysis decomposition and re-composition techniques were applied to extract the ~11 year signals in the hydrological records. An ~11 year cyclicity is evident in all eco-zones but it is superimposed by non-periodic variability in the 2 to 18 year wavebands that are due to El Nino/Southern Oscillation and North Atlantic Oscillation related precipitation variability or random components in the records. The ~11 year MAS cyclicity is strong in the Mountain ecozone (Rocky Mountains) and less strong in the Boreal Shield. In these eco-zones, it was found that years that experienced major floods were most likely to occur during low sunspot number years, in the spring time approximately 6–7 years after the last solar maximum. The results of the wavelet analysis demonstrate that major floods are more likely to occur during sunspot cycles with relatively low sunspot numbers after the last maximum.

© 2012 Elsevier B.V. All rights reserved.

1. Introduction

The influence of variability in the solar irradiance and galactic cosmic ray flux on the surface temperature and precipitation variability of the Earth has often been considered negligible because the sun's output varies by only ~0.1% on decadal time scales which can account for a global average temperature change of ~0.1 K (Eddy, 1976). Recently, however, Svensmark and Friis-Christensen (1997) found that the fluctuation in the cosmic ray flux can be directly related to increases of aerosols and ion-charged raindrops, which in turn are responsible for an increase in cloud cover during times of increased cosmic flux, and potentially higher precipitation. Observational records of global cloud cover and cosmic ray counts have been found to have a negative correlation with the solar irradiance flux over 11 year sunspot cycles (Marsh and Svensmark, 2000).

A number of other studies have explored the influence of solar activity on regional climate time series. Wang et al. (2003) found that the length of the solar cycle may be a useful indicator for droughts and floods in China, Alexander et al. (2007) found that

a statistically significant 21 year periodicity is present concurrently in South African annual rainfall, river flow, and lake levels and the Southern Oscillation Index, Juan and Yanben (2005) found that solar activity influenced precipitation in Beijing, and Perry (2007) found evidence of a physical linkage between galactic cosmic rays and regional climate time series in the Midwestern United States. The influence of long-term solar activity on streamflow has also been demonstrated in several recent studies by Mauas et al. (2005, 2008, 2011).

Several studies have disputed the influence and forecast potential of the 11 year solar cycle on decadal re-occurrences of streamflow extremes such as flood events (for example Reddy et al., 1989; Timoney et al., 1997). These studies generally focus on the relationships in wavelength and phase. Furthermore, the regional and temporal stationarity of 11 year solar and hydrological cycles is questioned (e.g., Currie and O'Brien, 1988). These studies do not discuss the relationships between the magnitudes of solar cycles and flood events. Moreover, the ~11 year sunspot cycles vary over time (averaging ~10.5 years), and exhibit large variations in their magnitude throughout the second half of the 20th century (Friis-Christensen and Lassen, 1991). In addition, solar activity variability such as in the ~11 year band is not translated linearly into climate and streamflow change but likely through a series of non-

---

* Corresponding author. Tel.: +1 514 398 7786.
    E-mail address: jan.adamowski@mcgill.ca (J. Adamowski).

linear oceanic-atmospheric responses, such as solar-intensity influence pressure anomaly perturbations and changing wind regimes (e.g., Hameed and Lee, 2005). There is also concern that 11-year streamflow cyclicity may spuriously arise from random or non-linear processes as demonstrated by a study of the Nile flood record in Egypt (for example Hurst, 1951; Koutsoyiannis, 2006).

One of the objectives of this study is to provide a better understanding of the potential link between 11 year sunspot cyclicity and the re-occurrence of large instant floods in multi-year time intervals. Most streamflow records are too short to determine the statistical significance of the average amplitudes (or spectral power) and stationarity (i.e. constant wavelength) of the detected periodicities. In this study, continuous wavelet analysis (Morlet et al., 1982) is used to extract wavelengths, magnitudes and phases of potential ~11 year (9–13 years) solar cyclicity. In contrast to Fourier analysis, continuous wavelet analysis (CWT) allows one to extract and reconstruct varying amplitudes, phases and wavelengths in streamflow records thus allowing one to link them precisely to the same parameter of variability of the ~11 year solar cycle. The testing of the extracted 11 year signal with varying amplitudes and slightly varying wavelengths is based on correlation with the 11 year cycle, and not on test versus randomness as done with Fourier analysis.

Wavelet analysis has recently been used to detect interruptions in climate trends and cycles, as well as to trace rainfall variability (e.g., Nakken, 1999), solar irradiance, and inter-decadal climate oscillations (e.g., Oh et al., 2003; Lucero and Rodriguez, 2000). A study using an entropy spectral technique found evidence of an 11 year sunspot cycle and Indian rainfall correlation (Reddy et al., 1989), but did not explain the temporal variability in the time lag or the strength of this linkage. Continuous wavelet analysis is a method that allows one to extract and reconstruct varying amplitudes, phases and wavelengths in streamflow records and to link them precisely to the variability of the ~11 year solar cycle, in contrast to Fourier or trend analysis based methods.

This study aimed at defining the geographic frame at which solar cyclicity can be used to forecast years with extreme flood events. Another objective was to provide a methodology to assess the risks of floods related to quasi-periodic, precipitation-related, and natural variability such as solar intensity cyclicity.

2. Data

The hydrological data used in this study were extracted from the Reference Hydrometric Basin Network (RHBN) data sets established by Environment Canada (1999). This data provides a significant amount of scientific information including over a hundred records of annual maximum flows from Canadian watersheds. Most of these records are short (<20 years) or from watersheds that are significantly altered or influenced by dams, canals or agricultural activity. Canada has been divided into 18 eco-zones based on vegetation, wildlife, latitude, altitude, proximity to oceans, terrain, and other criteria (Environment Canada, 1999).

In this study, data from six 'pristine' (minor or no human influence) rivers across Southern Canada were analyzed, spanning four eco-zones over a distance of about 5000 km from the Atlantic to the Pacific (Fig. 1, Table 1). These six data sets have the advantage that they contain data for a relatively long time period of a minimum of 40 years, and represent watersheds that have experienced no or only minor human influence (i.e. engineering, dams, agriculture, etc.). Statistical tests based on the recommendations of Shiau and Condie (1980) were carried out to verify the quality of the data (Environment Canada, 1999). Most of the maximum annual flows (MAS) have been measured for each year, but measurements are
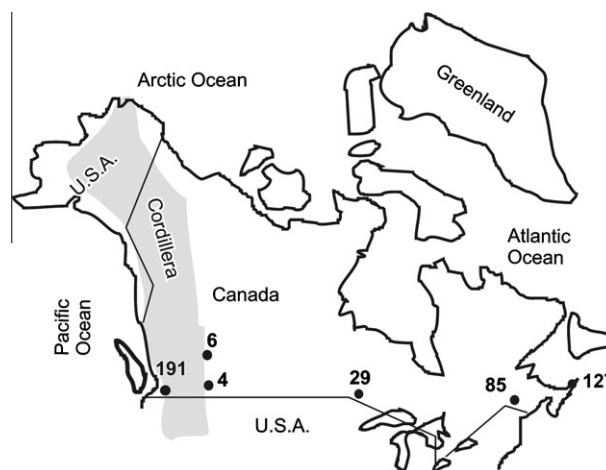

Fig. 1. Map of Canada with streamflow sample locations covering all the Southern Canadian eco-zones (see Table 1).

Table 1
Location and numbers of years of instant flow measurements.

Station ID	Name of station	Latitude degree N	Longtitude degree W	Drainage area (km²)	Ecozone
4	Belly river near mountain view	49.1000	113.6967	319	Montane Cordillera
6	Bow river at BANFF	51.1750	115.5694	2210	Montane Cordillera
29	Turtle river near mine centre	48.8500	92.7250	4870	Boreal Shield
85	Saint john river at fort kent	47.2569	68.5931	14,700	Atlantic Maritime
127	Northeast Margaree river at Margaree valley	46.3694	60.9767	368	Atlantic Maritime
191	Chilliwack river at outlet of chilliwack L.	49.0839	121.4567	329	Pacific Maritime

missing for single or several years for some stations (Fig. 2). Records of sunspot data since 1750 were collected from the NOAA web page (http://www.giss.nasa.gov/data/simodel/solar.irradiance/). In this study, part of the sunspot number record was used which corresponded to the same time interval as the streamflow records (Fig. 3A).

3. Methods

3.1. Signal decomposition using the continuous wavelet transform

Wavelet analysis (WA) is a filtering and data compression method that has been used since the 1980's (e.g., Morlet et al., 1982), and which can automatically detect and localize periodic signals, gradual shifts and abrupt interruptions in time, such as in streamflow records (e.g., Adamowski, 2008a, 2008b; Adamowski et al., 2009). Wavelet transforms use narrow analysis windows at high frequencies, and wide analysis windows at low frequencies, while Fourier analysis, the maximum entropy spectral technique, or Sliding-Window Fourier transform analysis use a single analysis window or shifting analysis windows of constant width, respectively (Rioul and Vetterli, 1991). The scaling properties of WA allows for the detection and extraction of temporal variability in
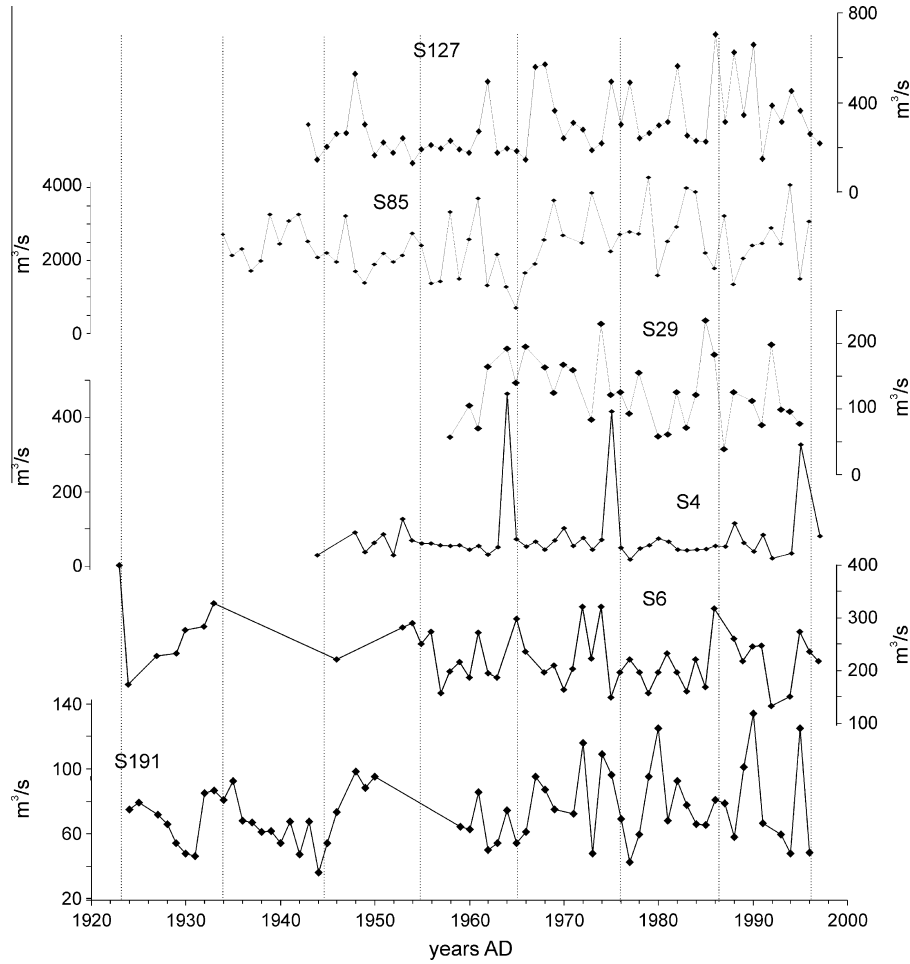
Fig. 2. Maximum annual streamflow (MAS) measurements (in m³/s) in Southern Canada from 1923 to 1997 ordered from East (top) to West (bottom). Note: Available measurements are marked with a diamond symbol. Dotted vertical lines mark 10.5 year intervals.

selected wavebands, which is an issue of particular interest in this study. The wavelet coefficients W of a time series $x(s)$ with s referring to distance of, as in this study, time, are calculated by the convolution

$$W_\psi(a,b) = \left(\frac{1}{\sqrt{a}}\right) \int_{-\infty}^{\infty} x(s)\psi\left(\frac{s-b}{a}\right) ds \qquad (1)$$

where ψ is the mother wavelet; the variable a is the scale factor that determines the characteristic frequency or wavelength; and b represents the shift of the wavelet over $x(s)$ (Chao and Naito, 1995). The wavelet coefficients W are normalized to represent the amplitudes of Fourier frequencies by replacing $\sqrt{a}$ with a. The matrix of wavelet coefficients $W(a,b)$ form the so called 'scalogram', which is coded with shades of gray or colors for graphical expression.

In this study, the continuous wavelet transform with the Morlet wavelet as the mother function was used, which is simply a sinusoid with the wavelength/period a modulated by a Gaussian function (Morlet et al., 1982). A parameter l is used to modify the wavelet transform bandwidth resolution either in favor of time or in favor of frequency, because the bandwidth resolution for the wavelet transform varies with frequency resolution $\Delta a = \frac{\sqrt{2}}{4\pi a l}$ with Δa referring to dilation in scale (or wavelength), and a location resolution $\Delta b = \frac{al}{\sqrt{2}}$ with Δb referring to dilation in time (or time-steps). For all analyzes $l = 6$ was chosen, which gives sufficiently precise results in the resolution of depth and frequency, respectively (Ware and Thomson, 2000). The shifted and scaled Morlet mother wavelet that was used is defined as

$$\psi_{l,a,b}(s) = \sqrt[4]{\pi}\sqrt{al}\, e^{-\frac{i2\pi(s-b)}{a}} e^{-\frac{1}{2}\left(\frac{s-b}{al}\right)^2} \qquad (2)$$

The wavelet analysis technique used in this article is explained in Prokoph and Barthelmes (1996).

The wavelet coefficients at the beginning and end of the data are subject to 'edge effects' because parts of the analysis windows are located outside of the data set. For the large analysis windows that are used for long wavelengths most of the analysis window can be located outside the range of the time series. Thus, the edge effects of the wavelet coefficients have a curved shape in the time frequency space, which is called the 'cone of influence' (Torrence and Compo, 1998). The edge effects have been compensated for by a normalization approach that is described in Adamowski et al. (2009).

Wavelet coefficients (i.e. amplitudes) and phases were extracted for the 8–13 year waveband of the streamflow records to evaluate the particular effect of this waveband on the overall streamflow data variability and its potential relation to $\sim$11 year solar insulation variability. This is shown in the example for wavelet analysis of station S4 (Fig. 3B–D).

3.2. Reconstruction of the $\sim$11 year wavelength components

The original time series can be completely reconstructed using the inverse wavelet transform (Grossman and Morlet, 1984; Holschneider et al., 1989)

$$x(s) = \int_0^{a\,\max} \int_0^{b\,\max} W_a(b)\Psi\left[\frac{(s-b)}{a}\right] db\frac{da}{a^2} \qquad (3)$$
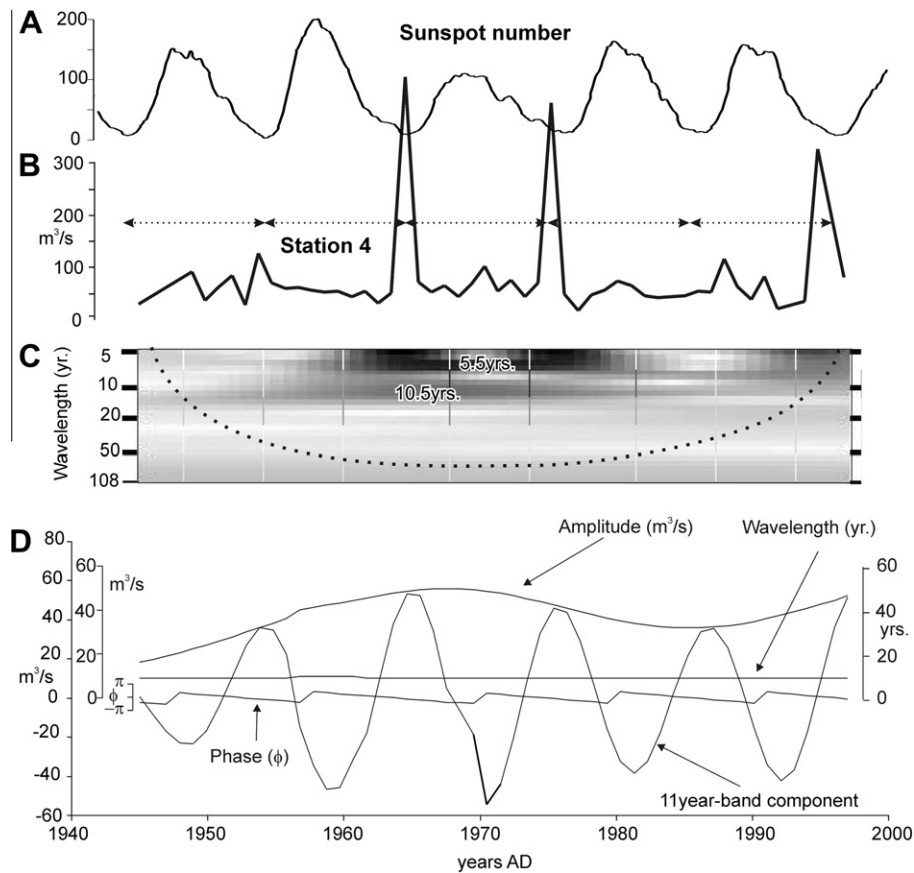
Fig. 3. Wavelet analysis of annual maximum streamflow of station 4 using Morlet wavelet. A: Monthly sunspot numbers from 1942 to 2000 (NOAA, 2008) for comparison. B: Annual maximum streamflow data (in m³/s) from station 4 with double-ended arrows marking the average mid-20th century sunspot cycle interval of 10.5 years. C: Scalogram of continuous wavelet analysis (CWT) of MAS record of station 4. Vertical axis: wavelength (or scale) in years. Strong signals are characterized by dark grey to black shades, and weak or absent signals are marked by light-grey to white shades. The dotted curved line marks the cone of influence. D: Wavelength (in years) with the largest amplitude, i.e. wavelet coefficient (in m³/s) and the phase (in radians) of this signal at any time in the 8–13 year waveband, as well as the reconstruction (in m³/s) of the ~11-year (8–13 years) component from the phase, amplitude and wavelength for any date (scale on far left). For details on decomposition and reconstruction see text.

In this study only signals from the ~11 (8–13) year waveband were of interest for reconstruction. Thus, the reconstruction was reduced to narrow wavebands da (8, 13 years) for a single component centred at $a = 11$ years from the start of the time series set at $b = 0$ to its end b_{max}. The reconstructed data interval db is set to $db = 1$ year. Thus, the partial reconstruction in the (8, 13) year waveband results in the component time series $x_a(s)$ as shown by

$$x_a(s) = \int_0^{b\,max} W_a(b)\Psi\left[\frac{(s-b)}{a}\right]db \qquad (4)$$

The reconstructions of signal $x(s)$ of component a were further simplified by the inclusion of phase φ at each time s for waveband centered at a in the reconstruction equation

$$x_a(s) = W_a(b)(\cos 2\pi s/a + \phi_a(s)) \qquad (5)$$

with φ representing the phase at time s. The partition of variability contributed by the 11-year cyclicity can be documented by reconstructing the ~11 year waveband and subtracting it from the complete records.

4. Results

Visual inspection indicates that the maximum annual streamflow (MAS) records appear to only occasionally follow a sharp 10.5 year re-occurrence pattern, such as can be seen in station S4 from 1964 to 1975 (Fig. 2). Moreover, the MAS variability is in general much higher in Atlantic Canada (for example station S85) than in South-Central Canada (Station S29).

The variability results in a series of short and long term cyclicities, from which the ~11 year cyclicity emerges as the most persistent, but not always the strongest cylicity in the MAS records (Fig. 4). With the exception of the near Pacific coast station S191, all other stations exhibit strong MAS fluctuations of ~4–6 year wavelength in the 1960s and 1970s (Fig. 4A–D). This cyclicity is however non-persistent, and vanishes later or is replaced by a weaker ~8 year cyclicity.

The 11 year cyclicity is also relatively insignificant at station S127 (Atlantic coast) which has much stronger cyclicities in the sub-decadal band (<10 years) and in the >20 year waveband. Multi-decadal signals of >20 year wavelengths are strong in both records from the Atlantic Region but become gradually weaker towards the West. These cycles are likely related to the changing precipitation patterns that evolve from the influence of the North Atlantic Oscillation (NAO). The percentage of variance related to the 11-year cycle ranges from ~4% to 25% for the 6 sections (Table 2). The amplitudes of the 11 year MAS cycle vary by factors of 1.5 (S6) to 2.5 (S127) from around 1920 to 2000. In comparison, the 11 year cycle of the sunspot number varies by a factor of 2.5 (Fig. 5). Moreover, the amplitude variability of the solar cycle is roughly negatively correlated to the amplitude variability of the ~11 year MAS cycles of stations S4 and S6 from the Montane Cordillera eco-zone, and S127 from the Atlantic Maritime eco-zone. The amplitude variability at the other stations shows no obvious relationship to the solar cycle amplitude variability.
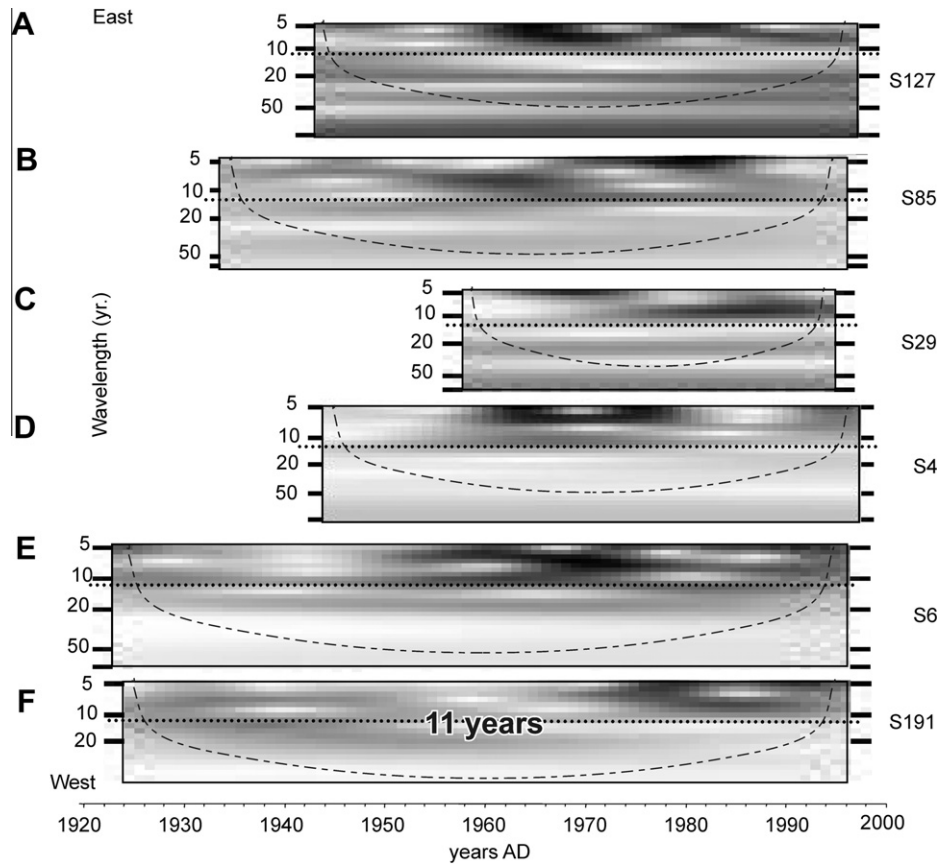
Fig. 4. Wavelet scalograms of MAS records from six Canadian Rivers. Note: Signal intensity increasing linearly from white to black; horizontal dotted lines mark 11 year wavelength location; curved stripped lines mark cones of influence with strong signal intensity.

The complete reconstruction of the ~11 year signals in the MAS records shows very similar patterns for the Montane Cordillera ecozone (S4 and S6 in Fig. 6). The phase offsets of these 11 year MAS records as well as the record of S29 to the previous sunspot maxima is ~5–7 years (Fig. 6, Table 2). Floods in the Montane and Boreal watersheds always occur during the spring. This can result in several months of variability in the offset to the last sunspot maxima. 60% Of the Montane Cordillera eco-zone MAS records and 25% of the Boreal Shield eco-zone long-term maxima in MAS (see Fig. 2) were able to be reconstructed at annual accuracy (Table 2). In contrast, none of the long-term maxima in MAS from the Atlantic Maritime eco-zone (S85 and S127), and only one maxima from the Pacific eco-zone (S191) could be lined up exactly with the solar cycle using the calculated phase shifts (Table 2). Despite the occasional good visual correspondence between flow peak and sunspot

minima or maxima (Fig. 2), there is no significant linear correlation between solar and flow records. The linear correlation becomes >95% significant for the 11-year flow component and sunspot after applying the offset determined via wavelet analysis (Table 2).

5. Discussion

The results of this study suggest that solar radiation variability at ~11 year periodicity contributes to changes in the multi-annual MAS pattern in the Montane Cordillera eco-zone, and possibly in the Boreal Shield (Central Canada). The ~11 year MAS cyclicity is much more subdued along the Atlantic and Pacific coasts, where 2–8 year and >20 year MAS cycles dominate. This observation confirms reports of ~18–30 year cycles in precipitation and large river

Table 2
Comparison of 11-year cycle of maxima of annual flow and solar variability.

Station ID	Years measured[b]	Variance raw data	Variance 11-year cycle removed	% Variance removed	Offset (yr) flood after LSM[b]	% Correct peak forecast	r Comp. at offset[c]
4	49	7600	6812	10.37	6.0	60	0.62
6[a]	43[a]	2449	2160	11.80	7.0	60	0.69
29	32	2646	1983	25.06	5.0	25	0.73
85	61	635,591	575,449	9.46	–	0	
127	55	21,307	20,403	4.24	–	0	
191	61	468	421	10.04	1.0	16	0.82

[a] 1953–1997 only.
[b] LSM Last Sunspot Maximum.
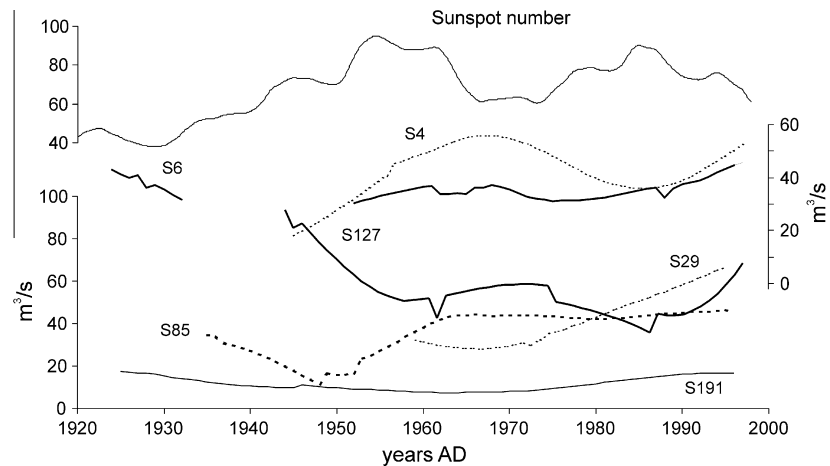[c] 99% Confidence at $r > 0.41$.

Fig. 5. Comparison of changes of amplitudes of ~10.5 year sunspot cycle (top panel) derived from monthly sunspot number fluctuations (see Fig. 3A) and of amplitudes of ~10.5 year cycles of MAS records in Southern Canada from 1920 to 1997. For station ID's see Table 1. Note that the missing record for station 6 from 1932 to 1950 corresponds to a gap in its amplitude graph.
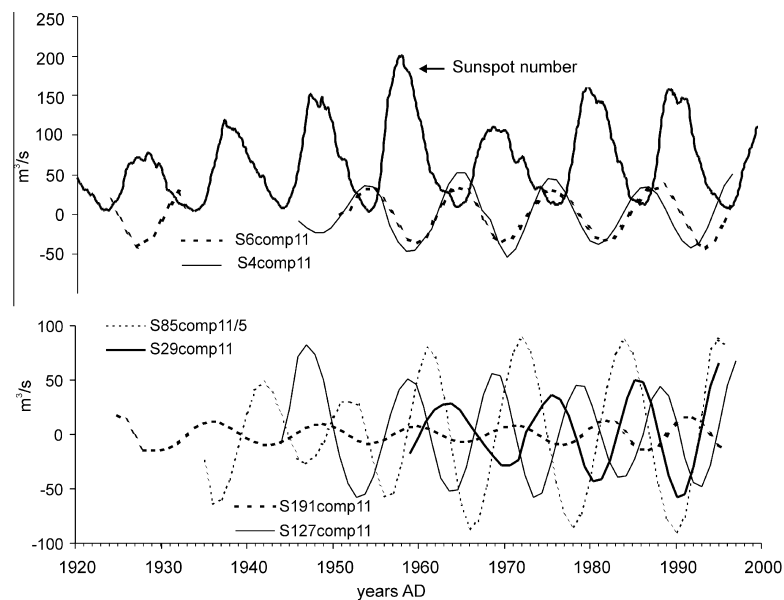

Fig. 6. Reconstruction of the ~11-year component of the MAS records (in m³/s) from Southern Canada with comparison to the monthly sunspot number variation. Top panel: 11-year components from the stations from the Montane Cordillera (Rocky Mountain foothills) with good signal stationarity and significant negative correlation to sunspot fluctuations. Bottom panels: 11-year components from other Canadian stations with poor signal stationarity and insignificant correlation to sunspot fluctuations (see Table 2). Note: The amplitude of the record from station 85 is scaled to 1/5 for presentation purposes.

discharges following the NAO/Southern Oscillation Index (SOI) change pattern along the coastlines (Currie and O'Brien, 1988; Pekárová et al., 2003; Labat et al., 2005). Wavelet analysis by Labat et al. (2005) also confirmed our observation that the NAO pattern influence varies temporally, being most strongly represented in the river discharge pattern around 1970. Cycles of 2–8 years are also commonly found in drought, precipitation and river discharge in North America and are commonly related to the El Nino/Southern Oscillation (ENSO) pattern (Oladipo, 1989; Gingras and Adamowski, 1995; Labat et al., 2005; Tardif et al., 1998). The weak 11 year precipitation cycle in Eastern Canada and the North East United States (Currie et al., 1988; Tardif et al., 1998) likely caused the weak ~11 year MAS cycle in the Atlantic Maritime eco-zones. The results demonstrate that the persistent and robust bandwidth of the 11-year solar cycle over the previous couple of centuries al-

lows one to relate streamflow signals in the same bandwidth even if the amplitudes vary. This method cannot be applied to relate ENSO, NAO or other oceanic-atmospheric systems to streamflow signals because their wavebands are not as narrow and persistent as the 9–12 year solar cycles.

The well pronounced 11 year MAS cyclicity in the Montane Cordillera eco-zone can be explained by the dominance of the solar radiation variability over the NAO and ENSO influence away from the oceanic coastlines. The low in sunspot and solar radiation every 11 years leads to higher amounts of cosmic rays hitting the Earth's atmosphere, which leads to more clouds and higher precipitation (Carslaw et al., 2002). Observational data indicates that changes in cloud cover during the peak of an 11-year sunspot cycle results in temporal precipitation changes, although with regional differences (Meehl et al., 2009). Higher precipitation during 11 year sun-

spot lows have also been detected in the Canadian Prairies (Garnett et al., 2006), which likely results in correspondingly higher flow levels in the two stations located on the Eastern Rocky Mountain/Prairies transition (foothills) where the significant sunspot influence had been detected.

The output of solar ultraviolet (UV) radiation varies by up to 4% during a typical 11-year solar cycle (in the 240–320 nm region) compared to the ~1% average solar energy fluctuations in the same cycle period (Lean, 2000; Gray et al., 2010). Thus, in particular, Montane regions that already receive more UV radiation in general than lowlands may receive significantly less solar energy as well as more precipitation due to more clouds during solar low years. This leads to more albedo, snow accumulation and a later but more abrupt onset of snowmelt and stronger floods in the year. The resulting precipitation cyclicity is likely enhanced by a positive feedback with (longer) snow accumulation and abrupt spring melt that leads to periodic 11 year floods in the Rocky Mountain region (Timoney et al., 1997). The maximum floods appear most often (~60%) during years with minimum sunspot numbers or one year before, about 4 years before the next and 7 years after the last sunspot maximum (Figs. 2, 3 and 6). The results of wavelet analysis also suggest that the maximum floods during an MAS cycle are stronger when the 11 year sunspot cycle is weaker. The number of records is too low to address significant risks for floods in the Montane Cordillera at minimum sunspot number years, but policy makers and water managers are advised to observe streamflows in this eco-zone more carefully during these episodes. Similarly, the observed high MAS during sunspot minima in Central Canada from a single, incomplete streamflow record (Figs. 2 and 6) cannot be considered significant enough to address the risk statistically. It is recommended that policy makers and other researchers carry out additional data analysis on the potential solar-flood link in this region as the Boreal Shield and the Great Plain cover large parts of North America. However, there is no long-term trend that is evident in the Montane eco-zone that could be related to long-term climate change.

6. Conclusions

The MAS in watersheds in Southern Canada can be related to 11 year solar cyclicity in regionally varying degrees. An approximately 11 year cyclicity is evident in all eco-zones but it is superimposed by much stronger NAO and ENSO related precipitation variability. The 11 year MAS cyclicity is strong in the Montane eco-zone (Rocky Mountains) and less significant in the Boreal Shield. In these eco-zones, high MAS (main floods) will most likely occur during low sunspot number years. The MAS are generally higher during weaker sunspot cycles.

Acknowledgment

References

Adamowski, J., 2008a. Development of a short-term river flood forecasting method for snowmelt driven floods based on wavelet and cross-wavelet analysis. Journal of Hydrology 353, 247–266.

Adamowski, J., 2008b. River streamflow forecasting using wavelet and cross-wavelet transform models. Journal of Hydrological Processes 22, 4877–4891.

Adamowski, K., Prokoph, A., Adamowski, J., 2009. Development of a new method of wavelet aided trend detection and estimation. Hydrological Processes 23, 2686–2696.

Alexander, W.J.R., Bailey, F., Bredenkamp, D.B., van der Merwe, A., Willemse, N., 2007. Linkages between solar activity, climate predictability and water resource development. Journal of the South African Institution of Civil Engineering 49, 32–44.

Carslaw, K.S., Harrison, R.G., Kirkby, J., 2002. Cosmic rays, clouds, and climate. Science 298, 1732–1737.

Chao, B.F., Naito, I., 1995. Wavelet analysis provides a new tool for studying Earth's rotation. EOS 76, 164–165.

Currie, R.G., O'Brien, D.P., 1988. Periodic 18.6 year and cyclic 10–11 year signals in Northeastern United States precipitation data. Journal of Climatology 8, 255–281.

Eddy, J.A., 1976. The Maunder minimum. Science 192, 1189–1202.

Environment Canada, 1999. Establishment of the Reference Hydrometric Basin Network (RHBN) for Canada. Environment Canada, Ottawa, p. 42.

Friis-Christensen, E., Lassen, K., 1991. Length of the solar cycle: an indicator of solar activity closely associated with climate. Science 254, 698–700.

Garnett, R., Nirupama, N., Haque, C.E., Murty, T.S., 2006. Correlates of Canadian prairie summer rainfall: Implications for crop yields. Climate Research 32, 25–33.

Gingras, D., Adamowski, K., 1995. The impact of El Nino oscillation on central Canadian floods and droughts. Canadian Journal of Civil Engineering 22, 834–837.

Gray, L.J., Beer, J., Geller, M., Haigh, J.D., Lockwood, M., Matthes, K., Cubasch, U., Fleitmann, D., Harrison, G., Hood, L., Luterbacher, J., Meehl, G.A., Shindell, D., van Geel, B., White, W., 2010. Solar influences on climate. Review of Geophysics 48, RG4001.

Grossman, A., Morlet, J., 1984. Decomposition of Hardy functions into square integrable wavelets of constant shape. SIAM Journal on Mathematical Analysis 15, 732–736.

Hameed, S., Lee, J.N., 2005. A mechanism for sun-climate connection. Geophysical Research Letters 32, L23817.

Holschneider, M., Kronland-Martinet, R., Morlet, J., Tchamitchian, P., 1989. A real-time algorithm for signal analysis with the help of the wavelet transform. In: Combes, J.M., Grossmann, A., Tchamitchian, P. (Eds.), Wavelets Time-Frequency Methods and Phase Space, Proceedings of the International Conference, Marseille, France, December 14–18, 1987. Springer-Verlag: Berlin; p. 286.

Hurst, H.E., 1951. Long term storage capacities of reservoirs. Trans. ASCE 116, 776–808.

Juan, Z., Yanben, H., 2005. Determination of precipitation cycle in Beijing area and comparison with solar activity cycle. Earth, Moon, and Planets 97, 69–78.

Koutsoyiannis, D., 2006. Nonstationarity versus scaling in hydrology. Journal of Hydrology 324, 239–254.

Labat, D., Ronchail, J., Guyot, J.L., 2005. Recent advances in wavelet analyses: Part 2 - Amazon, Parana, Orinoco and Congo discharges time scale variability. Journal of Hydrology 314, 289–311.

Lean, J., 2000. Evolution of the Sun's spectral irradiance since the Maunder Minimum. Geophysical Research Letters 27, 2425–2429.

Lucero, O.A., Rodriguez, N.C., 2000. Statistical characteristics of interdecadal fluctuations in the Southern Oscillation and the surface temperature of the equatorial Pacific. Atmospheric Research 54, 87–104.

Marsh, N., Svensmark, H., 2000. Low cloud properties influenced by cosmic rays. Physical Review Letter 85, 5004–5007.

Mauas, P.J.D., Flamenco, E., Buccino, A.P., 2008. Solar forcing of the stream flow of a continental scale South American river. Physical Review Letters 101, 168501.

Mauas, P.J., Buccino, A.P., Flamenco, E., 2011. Long-term solar activity influences on South American rivers. Journal of Atmospheric and Solar-Terrestrial Physics 73, 377–382.

Mauas, P.J., Flamenco, E., 2005. Solar activity and the streamflow of the Parana River. In: Ermolli, I., Pap, J., Fox, P. (Eds.), Solar Variability and Earth's Climate. Memoire Della Societa Astronomica Italiana – Series 76 (4), p. 1002–1003.

Meehl, G.A., Arblaster, J.M., Matthes, K., Sassi, F., van Loon, H., 2009. Amplifying the Pacific climate system response to a small 11-year solar cycle forcing. Science 325, 1114–1118.

Morlet, J., Arehs, G., Fourgeau, I., Giard, D., 1982. Wave propagation and sampling theory. Geophysics 47, 203–221.

Nakken, M., 1999. Wavelet analysis of rainfall-runoff variability isolating climatic from anthropogenic patterns. Environmental Modeling and Software 14, 283–295.

Oh, H.-S., Ammann, C.M., Naveau, P., Nychka, D., Otto-Bliesner, B.L., 2003. Multi-resolution time series analysis applied to solar irradiance and climate reconstructions. Journal of Atmospheric and Solar-terrestrial Physics 65, 191–201.

Oladipo, O.E., 1989. The quasi-periodic fluctuations in the drought indices over the North American Great Plains. Journal Natural Hazards 2, 1–16.

Pekárová, P., Miklánek, P., Pekár, J., 2003. Spatial and temporal runoff oscillation analysis of the main rivers of the world during the 19th–20th centuries. Journal of Hydrology 274, 62–79.

Perry, C.A., 2007. Evidence for a physical linkage between galactic cosmic rays and regional climate time series. Advances in Space Research 40, 353–364.

Prokoph, A., Barthelmes, F., 1996. Detection of nonstationarities in geological time series: Wavelet transform of chaotic and cyclic sequences. Computers and Geoscience 22, 1097–1108.

Reddy, R.S., Neralla, V.R., Godson, W.L., 1989. The solar cycle and Indian rainfall. Journal of Theoretical and Applied Climatology 39, 194–198.

Rioul, O., and M. Vetterli. 1991. Wavelets and signal processing. IEEE Special Magazine: 14–38.

Shiau, S.Y., Condie, R., 1980. Statistical Tests for Independence, Trend, Homogeneity, and General Randomness. Environment Canada, Inland Water Directorate, Ottawa.

Svensmark, H., Friis-Christensen, E., 1997. Variation of cosmic ray flux and global cloud coverage - a missing link in solar-climate relationships. Journal of Atmospheric and Solar-Terrestrial Physics 59, 1225–1232.

Tardif, J., Dutilleul, P., Bergeron, Y., 1998. Variations in periodicities of the ring width of black ash (Fraxinus Nigra Marsh.) in relation to flooding and ecological site factors at Lake Duparquet in Northwestern Québec. Biological Rhythm Research 29, 1–29.

Timoney, K., Peterson, G., Fargey, P., Peterson, M., McCanny, S., Wein, R., 1997. Spring ice-jam flooding of the Peace-Athabasca delta: evidence of a climatic oscillation. Climatic change 35, 463–483.

Torrence, C., Compo, G.P., 1998. A practical guide to wavelet analysis. Bulletin of the American Meteorological Society 79, 61–78.

Wang, Z., Feng, S., Tang, M., 2003. A relationship between solar activity and frequency of natural disasters in China. Advances in Atmospheric Sciences 20, 934–939.

Ware, D.M., Thomson, R.E., 2000. Interannual to multidecadal timescale climate variations in the Northeast Pacific. Journal of Climate 13, 3209–3220.